PERGAMON

International Journal of Solids and Structures 38 (2001) 7473–7485

INTERNATIONAL JOURNAL OF SOLIDS and STRUCTURES

www.elsevier.com/locate/ijsolstr

Dynamic behavior of a cylindrical crack in a functionally graded interlayer under torsional loading

Chunyu Li [a], George J. Weng [a,*], Zhuping Duan [b]

[a] *Department of Mechanical and Aerospace Engineering, Rutgers University, New Brunswick, NJ 8903, USA*

[b] *Laboratory of Nonlinear Mechanics, Institute of Mechanics, Chinese Academy of Sciences, 100080, People's Republic of China*

Received 27 June 2000

Abstract

In this paper the problem of a cylindrical crack located in a functionally graded material (FGM) interlayer between two coaxial elastic dissimilar homogeneous cylinders and subjected to a torsional impact loading is considered. The shear modulus and the mass density of the FGM interlayer are assumed to vary continuously between those of the two coaxial cylinders. This mixed boundary value problem is first reduced to a singular integral equation with a Cauchy type kernel in the Laplace domain by applying Laplace and Fourier integral transforms. The singular integral equation is then solved numerically and the dynamic stress intensity factor (DSIF) is also obtained by a numerical Laplace inversion technique. The DSIF is found to rise rapidly to a peak and then reduce and tend to the static value almost without oscillation. The influences of the crack location, the FGM interlayer thickness and the relative magnitudes of the adjoining material properties are examined. It is found among others that, by increasing the FGM gradient, the DSIF can be greatly reduced.

Keywords: Functionally graded materials; Dynamic stress intensity factor; Cylindrical crack; Torsional impact

1. Introduction

The interests in functionally graded materials (FGMs) research are growing rapidly in recent years. This is because the FGMs have many advantages, such as their high temperature and corrosion resistance, and their reductions in residual and thermal stresses. However, this kind of materials also brings up new problems. The foremost challenge is that the FGMs are inhomogeneous, with their material properties varying continuously. This inhomogeneity has a great influence on their mechanical behaviors. To face the challenge, considerable work has been embarked in recent years. These works can to some extent be seen from the review articles of Erdogan (1995), Tanigawa (1995) and Duan et al. (2001). It will be recognized from these reviews that only a few articles were devoted to the dynamic fracture mechanics of FGMs. Among these limited studies, Atkinson (1975) once considered crack propagation in media with spatially

* Corresponding author. Tel.: +1-732-445-2223; fax: +1-732-445-5313.
E-mail address: weng@jove.rutgers.edu (G.J. Weng).

0020-7683/01/$ - see front matter
PII: S0020-7683(01)00046-4

varying elastic moduli, and Wang and Meguid (1994/1995) treated a finite crack propagating in a inhomogeneous interlayer under an antiplane loading. Wang et al. (1998), on the other hand, carried out an analysis for a composite material with a material inhomogeneity in the thickness direction. In this process the continuously varying material is divided into a number of strips where each strip was assumed to be homogeneous. Babaei and Lukasiwicz (1998) studied a finite crack subjected to an antiplane shear impact load in an interlayer of a FGM between two dissimilar homogeneous bonding materials, while Li and coworkers (Li and Zou, 1999a; Li et al., 1999b) considered the dynamic responses of an FGM and an orthotropic FGM with a penny-shaped crack subjected to torsional impact.

In the present paper the problem of a cylindrical crack located in the FGM interlayer between two coaxial dissimilar homogeneous cylinders and subjected to a torsional impact loading is considered. We suppose that the two elastic homogeneous dissimilar cylinders are perfectly bonded through an elastic FGM layer and the shear modulus and the mass density of the FGM interlayer vary continuously between those of the two coaxial dissimilar homogeneous cylinders. We also assume that the external cylinder is infinite in radius. Although this is an idealized model for the purpose of obtaining an analytical solution, it actually has a background in the engineering practice. For example, in fiber-reinforced composite materials, there could be a thin inhomogeneous layer between the fiber and matrix. This interphase is formed either from the chemical reactions between the fiber and matrix materials or the use of a protective coating on the fiber during processing. It is the interphase that takes the role of insuring the fiber and matrix to cooperatively perform the function of the composite under the external load. Many studies (Achenbach and Zhu, 1989; Jasiuk and Kouider, 1993; Wacker et al., 1998; Ding and Weng, 1999) have shown that the interphase, either homogeneous or inhomogeneous, could significantly influence the overall mechanical behavior of the fiber-reinforced composites. However, the effect of the inhomogeneous interphase on the dynamic fracture behavior of a composite material has not been reported.

To solve the present problem we use the Laplace and Fourier integral transforms (Sneddon, 1972) and introduce a dislocation density function. The mixed boundary value problem is first reduced to a singular integral equation with a Cauchy type kernel in the Laplace domain. The resulting singular integral equation is then solved numerically following the method developed by Erdogan (1975). A numerical Laplace inversion technique described by Miller and Guy (1966) is subsequently used to obtain the dynamic stress intensity factor (DSIF) in the physical domain. The computational results are shown graphically to reveal the influences of the relative magnitudes of the adjoining material properties, the crack location, and the FGM interlayer thickness on the DSIF.

2. Formulation of the problem

As shown in Fig. 1, suppose that two elastic homogeneous dissimilar cylinders (material-I and material-III) are perfectly bonded through an elastic FGM layer (material-II). Material-I and material-III are coaxial and infinitely long and their material properties are constant and denoted by μ_1, ρ_1 and μ_3, ρ_3, where μ is the shear modulus and ρ is the mass density. Material-III is further assumed to be infinite in the radial direction. The FGM interfacial layer has the thickness of $c-a$ and its material properties are assumed to vary as

$$\mu_2(r)=\mu_0 r^m, \qquad \rho_2(r)=\rho_0 r^n. \tag{1}$$

From the continuity conditions of the material properties at the interfaces $r=a$ and $r=c$, i.e.

$$\begin{aligned} &\mu_2(a)=\mu_0 a^m=\mu_1, \qquad \rho_2(a)=\rho_0 a^n=\rho_1,\\ &\mu_2(c)=\mu_0 c^m=\mu_3, \qquad \rho_2(c)=\rho_0 c^n=\rho_3, \end{aligned} \tag{2}$$

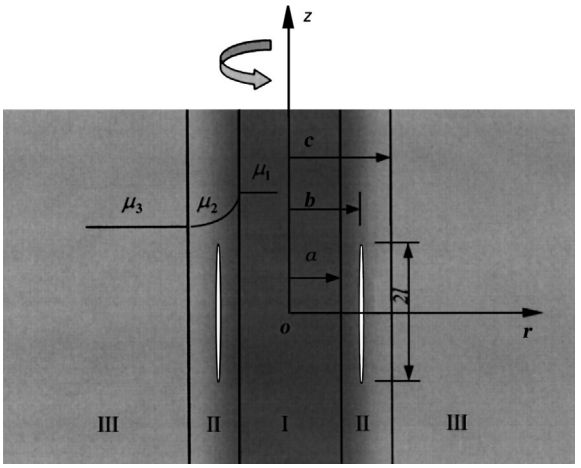

Fig. 1. A cylindrical crack in an FGM interlayer.

the parameters μ_0, ρ_0, m and n can be determined as

$$\begin{aligned} &\mu_0 = \mu_1/a^m, \qquad \rho_0 = \rho_1/a^n, \\ &m = \ln(\mu_3/\mu_1)/\ln(c/a), \\ &n = \ln(\rho_3/\rho_1)/\ln(c/a). \end{aligned} \tag{3}$$

Assume that a cylindrical crack of radius b and length $2l$ is located in the FGM interlayer (Fig. 1). Here, we only consider the Mode III crack problem. For simplicity, we assume that the crack surfaces are subjected to axisymmetric torsional impact loading $\tau(z)H(t)$, where $H(t)$ is the Heaviside unit step function, and the longitudinal shear stress $\tau(z)$ is symmetric about $z = 0$ plane. Considering the superposition theory of linear fracture mechanics, this loading condition yields the same stress intensity factor as an external torsional uniform stress imposed on the body.

Under present loading condition, by the cylindrical polar coordinates (r, θ, z), only the displacement $(u_\theta)_i = w_i(r, z, t)$ are nonvanishing, where subscripts $i = 1, 2, 3$ refer to materials I, II and III, respectively, and t represents the time. The nonvanishing stress components $\tau_{\theta z}$ and $\tau_{r\theta}$ are as follows:

$$(\tau_{\theta z})_i = \mu_i \frac{\partial w_i}{\partial z}, \qquad (\tau_{r\theta})_i = \mu_i r \frac{\partial}{\partial r}\left(\frac{w_i}{r}\right), \quad i = 1, 2, 3. \tag{4}$$

The governing equations of motion give

$$\frac{\partial^2 w_i}{\partial r^2} + \frac{1}{r}\frac{\partial w_i}{\partial r} - \frac{w_i}{r^2} + \frac{\partial^2 w_i}{\partial z^2} = \frac{\rho_i}{\mu_i}\frac{\partial^2 w_i}{\partial t^2}, \quad i = 1, 3, \tag{5}$$

$$\frac{\partial^2 w_2}{\partial r^2} + \frac{1+m}{r}\frac{\partial w_2}{\partial r} - \frac{1+m}{r^2} w_2 + \frac{\partial^2 w_2}{\partial z^2} = \frac{\rho_0}{\mu_0 r^{m-n}}\frac{\partial^2 w_2}{\partial t^2}. \tag{6}$$

The continuity conditions at the interfaces are

$$w_1(a^-, z, t) = w_2(a^+, z, t), \quad -\infty < z < \infty, \tag{7}$$

$$(\tau_{r\theta})_1(a^-, z, t) = (\tau_{r\theta})_2(a^+, z, t), \quad -\infty < z < \infty, \tag{8}$$

$$w_2(c^-, z, t) = w_3(c^+, z, t), \quad -\infty < z < \infty, \tag{9}$$

$$(\tau_{r\theta})_2(c^-,z,t) = (\tau_{r\theta})_3(c^+,z,t), \quad -\infty < z < \infty, \tag{10}$$

$$(\tau_{r\theta})_2(b^-,z,t) = (\tau_{r\theta})_2(b^+,z,t), \quad -\infty < z < \infty. \tag{11}$$

The boundary conditions at the crack surfaces are as follows:

$$w_2(b^+,z,t) = w_2(b^-,z,t), \quad l < |z| < \infty \tag{12}$$

$$(\tau_{r\theta})_2(b,z,t) = -\tau(z)H(t), \quad -l \leqslant z \leqslant l, \tag{13}$$

3. Displacements and stresses in the Laplace domain

Introducing the Laplace transform and defining

$$w_i^*(r,z,p) = \int_0^\infty w_i(r,z,t)\mathrm{e}^{-pt}\,\mathrm{d}t, \tag{14}$$

Eqs. (5) and (6) can be converted into

$$\frac{\partial^2 w_i^*}{\partial r^2} + \frac{1}{r}\frac{\partial w_i^*}{\partial r} - \frac{w_i^*}{r^2} + \frac{\partial^2 w_i^*}{\partial z^2} = \frac{\rho_i p^2}{\mu_i} w_i^*, \quad i = 1,3, \tag{15}$$

$$\frac{\partial^2 w_2^*}{\partial r^2} + \frac{1+m}{r}\frac{\partial w_2^*}{\partial r} - \frac{1+m}{r^2} w_2^* + \frac{\partial^2 w_2^*}{\partial z^2} = \frac{\rho_0 p^2}{\mu_0 r^{m-n}} w_2^*. \tag{16}$$

Further, introducing the pair of Fourier transforms,

$$V_i(r,\zeta,p) = \int_{-\infty}^\infty w_i^*(r,z,p)\mathrm{e}^{\mathrm{i}\zeta z}\,\mathrm{d}z, \tag{17}$$

$$w_i^*(r,z,p) = \frac{1}{2\pi}\int_{-\infty}^\infty V_i(r,\zeta,p)\mathrm{e}^{-\mathrm{i}\zeta z}\,\mathrm{d}\zeta, \tag{18}$$

the Eqs. (15) and (16) can be rewritten as

$$\frac{\partial^2 V_i(r,\zeta,p)}{\partial r^2} + \frac{1}{r}\frac{\partial V_i(r,\zeta,p)}{\partial r} - \left[\zeta^2 + \frac{\rho_i p^2}{\mu_i} + \frac{1}{r^2}\right] V_i(r,\zeta,p) = 0, \quad i = 1,3, \tag{19}$$

$$\frac{\partial^2 V_2(r,\zeta,p)}{\partial r^2} + \frac{1+m}{r}\frac{\partial V_2(r,\zeta,p)}{\partial r} - \left[\zeta^2 + \frac{\rho_0 p^2}{\mu_0 r^{m-n}} + \frac{1+m}{r^2}\right] V_2(r,\zeta,p) = 0. \tag{20}$$

Considering the displacement regularity conditions of w_1 at $r = 0$ and w_3 at $r \to \infty$, the solutions of Eq. (19) can be expressed as

$$V_1(r,\zeta,p) = A_1(\zeta,p)I_1(\gamma_1 r), \quad 0 \leqslant r < a, \tag{21}$$

$$V_3(r,\zeta,p) = A_6(\zeta,p)K_1(\gamma_3 r), \quad r > c \tag{22}$$

where

$$\gamma_1 = \sqrt{\zeta^2 + \frac{\rho_1 p^2}{\mu_1}}, \qquad \gamma_3 = \sqrt{\zeta^2 + \frac{\rho_3 p^2}{\mu_3}}. \tag{23}$$

and $I(\ )$, $K(\ )$ are the modified Bessel functions of the first and second kinds, respectively.

The solution to Eq. (20) will be given for two special cases. The first one is for $n = m$, and the second one for $n = m - 2$. The first case implies that the shear modulus and the mass density of the interphase change in the same way, but the second case allows them to change separately. The solutions of Eq. (20) at these two cases can be expressed in unified forms as

$$V_2(r,\zeta,p) = r^{-m/2}[A_2(\zeta,p)I_\beta(\gamma_2 r) + A_3(\zeta,p)K_\beta(\gamma_2 r)], \quad a < r < b, \tag{24}$$

$$V_2(r,\zeta,p) = r^{-m/2}[A_4(\zeta,p)I_\beta(\gamma_2 r) + A_5(\zeta,p)K_\beta(\gamma_2 r)], \quad b < r < c, \tag{25}$$

where

$$\beta = 1 + \frac{m}{2}, \qquad \gamma_2 = \sqrt{\zeta^2 + \frac{\rho_0 p^2}{\mu_0}}, \quad \text{when } n = m, \tag{26}$$

$$\beta = \sqrt{\left(1 + \frac{m}{2}\right)^2 + \frac{\rho_0 p^2}{\mu_0}}, \qquad \gamma_2 = \zeta, \quad \text{when } n = m - 2. \tag{27}$$

From Eqs. (18) and (21)–(25), we can obtain the displacements in the Laplace domain

$$w_1^*(r,z,p) = \frac{1}{2\pi}\int_{-\infty}^{\infty} A_1(\zeta,p)I_1(\gamma_1 r)\mathrm{e}^{-\mathrm{i}\zeta z}\,\mathrm{d}\zeta, \quad 0 \leqslant r < a, \tag{28}$$

$$w_2^*(r,z,p) = \frac{1}{2\pi}\int_{-\infty}^{\infty} r^{-m/2}[A_2(\zeta,p)I_\beta(\gamma_2 r) + A_3(\zeta,p)K_\beta(\gamma_2 r)]\mathrm{e}^{-\mathrm{i}\zeta z}\,\mathrm{d}\zeta, \quad a < r < b, \tag{29}$$

$$w_2^*(r,z,p) = \frac{1}{2\pi}\int_{-\infty}^{\infty} r^{-m/2}[A_4(\zeta,p)I_\beta(\gamma_2 r) + A_5(\zeta,p)K_\beta(\gamma_2 r)]\mathrm{e}^{-\mathrm{i}\zeta z}\,\mathrm{d}\zeta, \quad b < r < c, \tag{30}$$

$$w_3^*(r,z,p) = \frac{1}{2\pi}\int_{-\infty}^{\infty} A_6(\zeta,p)K_1(\gamma_3 r)\mathrm{e}^{-\mathrm{i}\zeta z}\,\mathrm{d}\zeta, \quad r > c. \tag{31}$$

Subsequently, the shear stresses $\tau_{\theta z}^*$ and $\tau_{r\theta}^*$ in the Laplace transform domain can be obtained from Eq. (4). The stress components $\tau_{r\theta}^*$ are listed as follows:

$$(\tau_{r\theta}^*)_1 = \mu_1 \frac{1}{2\pi}\int_{-\infty}^{\infty} \gamma_1 A_1(\zeta,p)I_2(\gamma_1 r)\mathrm{e}^{-\mathrm{i}\zeta z}\,\mathrm{d}\zeta, \quad 0 \leqslant r < a, \tag{32}$$

$$\begin{aligned}(\tau_{r\theta}^*)_2 = \mu_2(r) r^{-m/2}\frac{1}{2\pi}\int_{-\infty}^{\infty} &\{[-(1+m/2)I_\beta(\gamma_2 r)/r + \gamma_2 I'_\beta(\gamma_2 r)]A_2(\zeta,p) + [-(1+m/2)K_\beta(\gamma_2 r)/r \\ &+ \gamma_2 K'_\beta(\gamma_2 r)]A_3(\zeta,p)\}\mathrm{e}^{-\mathrm{i}\zeta z}\,\mathrm{d}\zeta, \quad a < r < b,\end{aligned} \tag{33}$$

$$\begin{aligned}(\tau_{r\theta}^*)_2 = \mu_2(r) r^{-m/2}\frac{1}{2\pi}\int_{-\infty}^{\infty} &\{[-(1+m/2)I_\beta(\gamma_2 r)/r + \gamma_2 I'_\beta(\gamma_2 r)]A_4(\zeta,p) + [-(1+m/2)K_\beta(\gamma_2 r)/r \\ &+ \gamma_2 K'_\beta(\gamma_2 r)]A_5(\zeta,p)\}\mathrm{e}^{-\mathrm{i}\zeta z}\,\mathrm{d}\zeta, \quad b < r < c,\end{aligned} \tag{34}$$

$$(\tau_{r\theta}^*)_3 = -\mu_3 \frac{1}{2\pi}\int_{-\infty}^{\infty} \gamma_3 A_6(\zeta,p)K_2(\gamma_3 r)\mathrm{e}^{-\mathrm{i}\zeta z}\,\mathrm{d}\zeta, \quad c < r < +\infty. \tag{35}$$

4. Derivation of the singular integral equation

In the Laplace domain, the boundary and interface conditions become

$$w_1^*(a^-,z,p) = w_2^*(a^+,z,p), \quad -\infty < z < \infty \tag{36}$$

$$(\tau_{r\theta}^*)_1(a^-,z,p) = (\tau_{r\theta}^*)_2(a^+,z,p), \quad -\infty < z < \infty, \tag{37}$$

$$w_2^*(c^-,z,p) = w_3^*(c^+,z,p), \quad -\infty < z < \infty, \tag{38}$$

$$(\tau_{r\theta}^*)_2(c^-,z,p) = (\tau_{r\theta}^*)_3(c^+,z,p), \quad -\infty < z < \infty, \tag{39}$$

$$(\tau_{r\theta}^*)_2(b^-,z,p) = (\tau_{r\theta}^*)_2(b^+,z,p), \quad -\infty < z < \infty, \tag{40}$$

$$w_2^*(b^-,z,p) = w_2^*(b^+,z,p), \quad l < |z| < \infty, \tag{41}$$

$$(\tau_{r\theta}^*)_2(b,z,p) = -\tau(z)/p, \quad -l \leqslant z \leqslant l. \tag{42}$$

In order to reduce the problem into an integral equation, we first define the following dislocation density function,

$$g(z,p) = \tfrac{\partial}{\partial z}\big[w_2^*(b^+,z,p) - w_2^*(b^-,z,p)\big], \quad -l \leqslant z \leqslant l. \tag{43}$$

Then substituting Eqs. (28)–(35) into the continuity conditions (36)–(40) and the dislocation density definition (43), and taking proper Fourier inverse transform and considering the Eq. (41), we can obtain six simultaneous equations for the six unknown functions $A_1(\zeta,p), A_2(\zeta,p), \ldots, A_6(\zeta,p)$ in terms of the unknown function g. Finally, substituting $A_4(\zeta,p)$ and $A_5(\zeta,p)$ into Eq. (34) and using the boundary condition (42), we obtain

$$\mu_2(b)b^{-m/2}\frac{1}{2\pi i}\int_{-\infty}^{\infty}\frac{1}{\zeta}\frac{\Delta_1(\zeta,p)}{\Delta(\zeta,p)}\int_{-l}^{l}g(s,p)e^{i\zeta(s-z)}\,ds\,d\zeta = -\frac{\tau(z)}{p} \tag{44}$$

after a complicated treatment, where $\Delta(\zeta,p)$ and $\Delta_1(\zeta,p)$ are listed in Appendix A.

Noting that

$$\lambda = \lim_{\zeta\to+\infty}\frac{1}{\zeta}\frac{\Delta_1(\zeta,p)}{\Delta(\zeta,p)} = \frac{b^{m/2}}{2}, \tag{45}$$

we can separate the singular part of the integral equation (44) by adding and subtracting λ from the integral kernel. Thus we obtain

$$\begin{aligned}&\frac{\lambda b^{-m/2}}{2\pi i}\int_{-\infty}^{\infty}\mathrm{sgn}(\zeta)\int_{-l}^{l}g(s,p)e^{i\zeta(s-z)}\,d\zeta\,ds + \frac{b^{-m/2}}{2\pi i}\int_{-l}^{l}\int_{-\infty}^{\infty}\left[\frac{1}{\zeta}\frac{\Delta_1(\zeta,p)}{\Delta(\zeta,p)} - \lambda\,\mathrm{sgn}(\zeta)\right]e^{i\zeta(s-z)}g(s,p)\,d\zeta\,ds\\ &= -\frac{\tau(z)}{p\mu_2(b)}.\end{aligned} \tag{46}$$

By using the formula of Riemann–Lebesgue (Churchill and Brown, 1978), we have

$$\int_{-\infty}^{\infty}\mathrm{sgn}(\zeta)\int_{-l}^{l}g(s,p)e^{i\zeta(s-z)}\,d\zeta\,ds = 2i\int_{-l}^{l}\frac{g(s,p)}{s-z}\,ds. \tag{47}$$

Considering the functions $\Delta(\zeta,p)$ and $\Delta_1(\zeta,p)$ are even functions about the variable ζ, we have

$$\int_{-\infty}^{\infty}\left[\frac{1}{\zeta}\frac{\Delta_1(\zeta,p)}{\Delta(\zeta,p)}-\lambda\,\mathrm{sgn}(\zeta)\right]\mathrm{e}^{\mathrm{i}\zeta(s-z)}\,\mathrm{d}\zeta=2i\int_0^{\infty}\left(\frac{1}{\zeta}\frac{\Delta_1(\zeta,p)}{\Delta(\zeta,p)}-\lambda\right)\sin(s\zeta-z\zeta)\,\mathrm{d}\zeta. \tag{48}$$

Substituting Eqs. (45), (47) and (48) into Eq. (46), we obtain a singular integral equation with a Cauchy kernel

$$\frac{1}{2\pi}\int_{-l}^{l}\frac{g(s,p)}{s-z}\,\mathrm{d}s+\frac{1}{\pi}\int_{-l}^{l}R(s,z,p)g(s,p)\,\mathrm{d}s=-\frac{\tau(z)}{p\mu_2(b)}, \tag{49}$$

where

$$R(s,z,p)=\int_0^{\infty}\left(\frac{b^{-m/2}}{\zeta}\frac{\Delta_1(\zeta,p)}{\Delta(\zeta,p)}-\frac{1}{2}\right)\sin(s\zeta-z\zeta)\,\mathrm{d}\zeta. \tag{50}$$

The single-valued condition of $g(s,p)$ can be given from the definition of $g(s,p)$,

$$\int_{-l}^{l}g(s,p)\,\mathrm{d}s=0. \tag{51}$$

5. Dynamic stress intensity factor

Following the numerical method for singular integral equations (Erdogan, 1975) and normalizing the integral interval by the following transformation of variables,

$$s=l\xi,\qquad z=l\eta, \tag{52}$$

the integral equations (49) and (51) can be rewritten as

$$\frac{1}{\pi}\int_{-l}^{l}\left[\frac{1}{2}\frac{1}{\xi-\eta}+\overline{R}(\xi,\eta,p)\right]G(\xi,p)\,\mathrm{d}\xi=-\frac{\overline{\tau}(\eta)}{p\mu_2(b)}, \tag{53}$$

$$\int_{-l}^{l}G(\xi,p)\,\mathrm{d}\xi=0, \tag{54}$$

where

$$\bar{R}(\xi,\eta,p)=lR(l\xi,l\eta,p), \tag{55}$$

$$G(\xi,p)=g(l\xi,p), \tag{56}$$

$$\overline{\tau}(\eta)=\tau(l\eta). \tag{57}$$

Considering the singularity at the crack tip, we assume that

$$G(\xi,p)=\frac{\overline{G}(\xi,p)}{p}\frac{1}{\sqrt{1-\xi^2}}. \tag{58}$$

Expanding $\overline{G}(\xi,p)$ in the forms of Chebyshev polynomials

$$\overline{G}(\xi,p)=\sum_{k=0}^{\infty}B_kT_k(\xi), \tag{59}$$

and using the properties of the polynomials, we obtain a system of equations,

$$\sum_{i=1}^{k}\left[\frac{1}{2}\frac{1}{\xi_i-\eta_j}+\bar{R}(\xi_i,\eta_j,p)\right]\frac{\overline{G}(\xi_i,p)}{k}=-\frac{\overline{\tau}(\eta_j)}{\mu_0 b^m}, \tag{60}$$

$$\sum_{i=1}^{k}\frac{\pi}{k}\overline{G}(\xi_i,p)=0, \tag{61}$$

where $i=1,2,\ldots,k$, $j=1,2,\ldots,k-1$ and ξ_i, η_j are the roots of the Chebyshev polynomials of the first and second kinds, respectively,

$$\begin{aligned}\xi_i&=\cos\left(\frac{2i-1}{2k}\pi\right),\quad i=1,2,\ldots,k,\\ \eta_j&=\cos\left(\frac{j}{k}\pi\right),\quad j=1,2,\ldots,k-1.\end{aligned} \tag{62}$$

After solving the system of linear algebraic equations (60) and (61), the unknown function $\overline{G}(\xi,p)$ can be obtained.

Defining the stress intensity factor in the Laplace domain as

$$K^*_{\mathrm{III}}(l,p)=\lim_{z\to l^+}\sqrt{2(z-l)}(\tau^*_{r\theta})_2(b,z,p), \tag{63}$$

$$K^*_{\mathrm{III}}(-l,p)=\lim_{z\to -l^-}\sqrt{2(-l-z)}(\tau^*_{r\theta})_2(b,z,p), \tag{64}$$

then from Eqs. (34), (45), (58) and (59) and using the following property of the Chebyshev polynomials (Erdogan and Wu, 1995)

$$\frac{1}{\pi}\int_{-l}^{l}\frac{T_k(\xi)\,\mathrm{d}\xi}{(\xi-\eta)\sqrt{1-\xi^2}}=\begin{cases}U_{k-1}(\eta), & |\eta|<1,\ k\geqslant 1,\\ -\frac{\eta}{|\eta|\sqrt{\eta^2-1}}\left(\eta-\frac{|\eta|\sqrt{\eta^2-1}}{\eta}\right)^k, & |\eta|>1,\ k\geqslant 0,\end{cases} \tag{65}$$

we obtain

$$K^*_{\mathrm{III}}(l,p)=-\frac{1}{2}\mu_0 b^m\sqrt{l}\frac{\overline{G}(1,p)}{p}, \tag{66}$$

$$K^*_{\mathrm{III}}(-l,p)=\frac{1}{2}\mu_0 b^m\sqrt{l}\frac{\overline{G}(-1,p)}{p}. \tag{67}$$

From the Laplace inversion

$$f(t)=\frac{1}{2\pi\mathrm{i}}\int_{\mathrm{Br}}f^*(p)\mathrm{e}^{pt}\,\mathrm{d}p, \tag{68}$$

where Br denotes the Bromwich path of integration, the DSIF in the time domain can be obtained by

$$K_{\mathrm{III}}(l,t)=-\frac{1}{2}\mu_0 b^m\sqrt{l}\frac{1}{2\pi\mathrm{i}}\int_{\mathrm{Br}}\frac{\overline{G}(1,p)}{p}\mathrm{e}^{pt}\,\mathrm{d}p, \tag{69}$$

$$K_{\mathrm{III}}(-l,t)=\frac{1}{2}\mu_0 b^m\sqrt{l}\frac{1}{2\pi\mathrm{i}}\int_{\mathrm{Br}}\frac{\overline{G}(-1,p)}{p}\mathrm{e}^{pt}\,\mathrm{d}p. \tag{70}$$

The Laplace inverse transformations in Eqs. (69) and (70) can be carried out by the numerical method provided by Miller and Guy (1966). For example, the function $\overline{G}(1,p)$ is first evaluated at some discrete points

$$p = (1+q)\delta, \qquad q = 0,1,2,\ldots, \tag{71}$$

then the Laplace inverse transformation can be approximately calculated by

$$\frac{1}{2\pi \mathrm{i}} \int_{\mathrm{Br}} \frac{\overline{G}(1,p)}{p} \mathrm{e}^{pt}\, \mathrm{d}p = \sum_{j=0}^{N-1} C_j P_j[2\exp(-\delta t) - 1], \tag{72}$$

where $P_j(\ )$ is the Legendre polynomial and the coefficients C_j are determined from the following equations

$$\frac{\overline{G}(1,(1+q)\delta)}{(1+q)} = \sum_{j=0}^{q} \frac{q(q-1)\ldots[q-(j-1)]}{(q+1)(q+2)\ldots(q+j+1)} C_j. \tag{73}$$

6. Results and discussion

To place the developed solutions in perspective, we now consider the cylindrical crack with a length $l/a = 1$ and a crack surface loading $\tau(z,t) = \tau_0 H(t)$. After solving the system of equations (53) and (54), and accomplishing the Laplace inversion (69) and (70) by the numerical procedure developed by Miller and Guy (1966), we obtain the DSIFs $K_{\mathrm{III}}(l,t)$ and $K_{\mathrm{III}}(-l,t)$ for several different cases of variations of μ_3/μ_1, c/a, b/a and ρ_3/ρ_1. In these numerical procedures, we take the number of integrating points $k = 31$ for the numerical solution of singular integral equations (53) and (54) and the parameters $\delta = 0.5$, $N = 6$ in the numerical procedure of Laplace inversion. Because of $\overline{G}(-1,p) = -\overline{G}(1,p)$ in this symmetric loading condition, we have $K_{\mathrm{III}}(-l,t) = K_{\mathrm{III}}(l,t)$ and then they are written as $K_{\mathrm{III}}(t)$. The results shown in Figs. 2–5 are the variations of the normalized DSIF $K_{\mathrm{III}}(t)/\tau_0\sqrt{l}$ with respect to $c_{21}t/l$, where $c_{21} = (\mu_1/\rho_1)^{1/2}$ is the shear wave velocity in material-I.

From Figs. 2–5 a general feature of the curves is observed: the DSIFs rise rapidly and reach a peak, then reduce gradually and tend to their respective static values. The peak values appear at about $c_{21}t/l = 2.0$ and are higher than their respective static values about 20%.

Fig. 2 shows the effect of crack position in the FGM interlayer, i.e. b/a, on the variation of the normalized DSIF $K_{\mathrm{III}}(t)/\tau_0\sqrt{l}$ with $c_{21}t/l$, at $\rho_3/\rho_1 = \mu_3/\mu_1 = 0.2$ and $c/a = 1.25$. It is observed that the $K_{\mathrm{III}}(t)/\tau_0\sqrt{l}$ tends to decrease monotonically with increasing b/a.

Fig. 3 displays the effect of FGM interlayer thickness, i.e. c/a, on the variation of $K_{\mathrm{III}}(t)/\tau_0\sqrt{l}$ while the crack is located at the position of $b/a = 1.15$ and $\rho_3/\rho_1 = \mu_3/\mu_1 = 0.2$. It indicates that the DSIF increases with increasing c/a. From $m = \ln(\mu_3/\mu_1)/\ln(c/a)$ of the Eq. (3), the increase of c/a implies the decrease of the absolute value of the exponent m. In other words the increase of c/a means the decrease of the material gradient. Thus we can conclude that increasing the FGM gradient is beneficial to the decrease of the DSIF.

The effect of the stiffness ratio μ_3/μ_1 on the variation of the DSIF is shown in Fig. 4. The other parameters are chosen as $c/a = 1.5$, $b/a = 1.15$ and $\rho_3/\rho_1 = \mu_3/\mu_1$. It can be seen that the $K_{\mathrm{III}}(t)/\tau_0\sqrt{l}$ increases when the ratio μ_3/μ_1 increases. For a definite value of c/a, the increase of μ_3/μ_1 from 0.2 to 1.0 results in a decrease of the absolute value of the exponent m. As such, we can also conclude that increasing the FGM gradient is helpful to the reduction of the DSIF. This conclusion is consistent with that deduced from Fig. 3.

Fig. 5 displays the effect of ρ_3/ρ_1 on the DSIF. The results for $\rho_3/\rho_1 = \mu_3/\mu_1$ are from the solvable case of gradient exponents $n = m$ and the results for $\rho_3/\rho_1 < \mu_3/\mu_1$ are from the solvable case of gradient exponents $n = m - 2$. It can be seen that the ratio of ρ_3/ρ_1 mainly has effect on the peak value of the DSIF

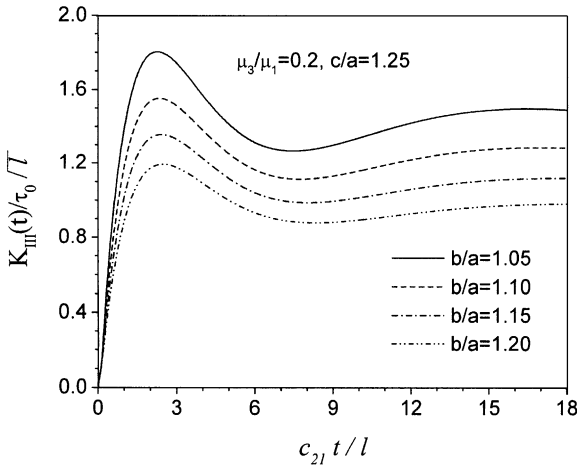

Fig. 2. The effect of the crack position on the normalized DSIF.

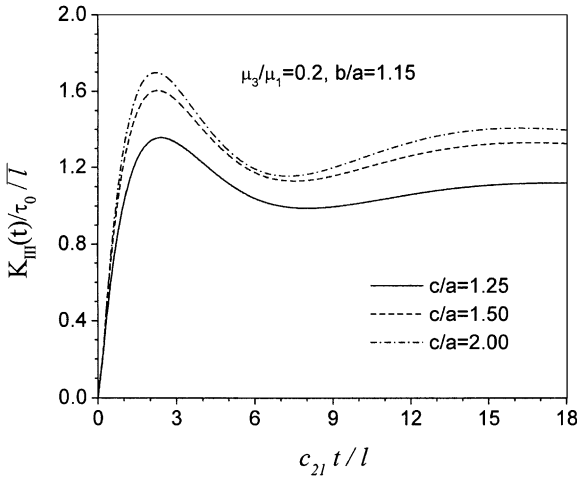

Fig. 3. The effect of the FGM interlayer thickness on the normalized DSIF.

and the decrease of ρ_3/ρ_1 results in the decrease of the peak value of DSIF. However, this effect is not significant.

7. Conclusions

This paper considers the problem of a cylindrical crack located in the FGM interlayer between two coaxial elastic dissimilar homogeneous cylinders under torsional impact loading. The shear modulus and the mass density of the FGM interlayer are assumed to vary continuously between those of the two coaxial cylinders. The dynamic elastic field and the DSIF are solved by using the techniques of integral transforms and singular integral equation. The DSIF is found to rise rapidly to the peak and then reduce and tend to the static value. The peak values are higher than their respective static values about 20%. The influences of the crack location, the FGM interlayer thickness and the relative magnitudes of the adjoining material prop-

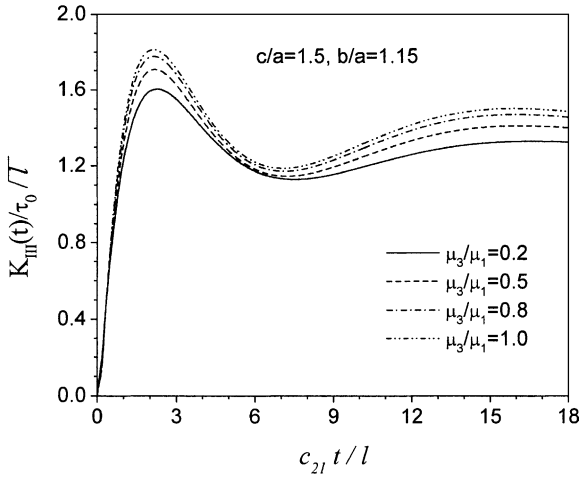

Fig. 4. The effect of the shear modulus ratio on the normalized DSIF.

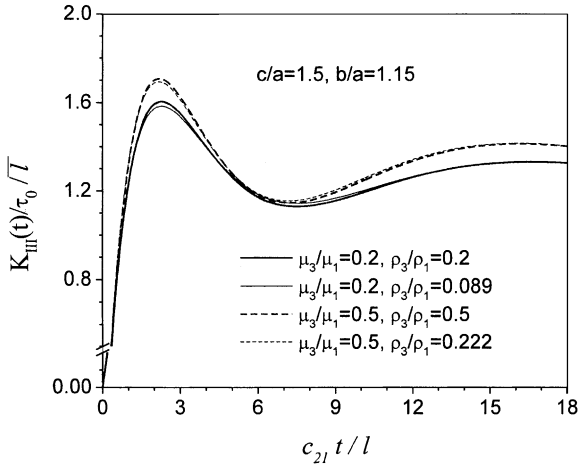

Fig. 5. The effect of the mass density ratio on the normalized DSIF.

erties are investigated. Three conclusions are deduced from the results: (i) the DSIF decreases when the cylindrical crack is far away from the axial center; (ii) the DSIF also decreases with decreasing thickness of the FGM layer; and (iii) the DSIF can be greatly reduced by increasing the gradient of the FGM; (iv) the peak value of DSIF can also be reduced by decreasing the difference of mass density of the adjoining materials.

Acknowledgements

This work was supported partially by the China Scholarship Council and partially by the National Science Foundation of USA under CMS-9625304. Z. Duan was supported by the National Natural Science Fund of China under the Key project no. 19891180.

Appendix A

The coefficients $\Delta(\zeta,p)$ and $\Delta_1(\zeta,p)$ in Eq. (43) are

$$\Delta(\zeta,p) = (d_{52}d_{61} - d_{51}d_{62})[(d_{21}d_{12} - d_{11}d_{22})(d_{32}d_{43} - d_{42}d_{33}) + (d_{11}d_{23} - d_{21}d_{13})(d_{31}d_{43} - d_{41}d_{33})]$$
$$\Delta_1(\zeta,p) = [d_{52}(d_{11}d_{22} - d_{21}d_{12}) - d_{51}(d_{11}d_{23} - d_{21}d_{13})][d_{51}(d_{32}d_{43} - d_{42}d_{33}) - d_{52}(d_{31}d_{43} - d_{41}d_{33})]$$

where

$$d_{11} = I_1(\gamma_1 a), \qquad d_{12} = -a^{-m/2}I_\beta(\gamma_2 a), \qquad d_{13} = -a^{-m/2}K_\beta(\gamma_2 a), \qquad d_{21} = \mu_1\gamma_1 I_2(\gamma_1 a),$$
$$d_{22} = -\mu_2(a)a^{-m/2}[-(1+m/2)I_\beta(\gamma_2 a)/a + \gamma_2 I'_\beta(\gamma_2 a)],$$
$$d_{23} = -\mu_2(a)a^{-m/2}[-(1+m/2)K_\beta(\gamma_2 a)/a + \gamma_2 K'_\beta(\gamma_2 a)],$$
$$d_{31} = c^{-m/2}I_\beta(\gamma_2 c), \qquad d_{32} = c^{-m/2}K_\beta(\gamma_2 c), \qquad d_{33} = -K_1(\gamma_3 c),$$
$$d_{41} = \mu_2(c)c^{-m/2}[-(1+m/2)I_\beta(\gamma_2 c)/c + \gamma_2 I'_\beta(\gamma_2 c)],$$
$$d_{42} = \mu_2(c)c^{-m/2}[-(1+m/2)K_\beta(\gamma_2 c)/c + \gamma_2 K'_\beta(\gamma_2 c)],$$
$$d_{43} = \mu_3\gamma_3 K_2(\gamma_3 c),$$
$$d_{51} = -(1+m/2)I_\beta(\gamma_2 b)/b + \gamma_2 I'_\beta(\gamma_2 b),$$
$$d_{52} = -(1+m/2)K_\beta(\gamma_2 b)/b + \gamma_2 K'_\beta(\gamma_2 b),$$
$$d_{61} = b^{-m/2}I_\beta(\gamma_2 b), \qquad d_{62} = b^{-m/2}K_\beta(\gamma_2 b).$$

References

Achenbach, J.D., Zhu, H., 1989. Effect of interfacial zone on mechanical behavior and failure of fiber-reinforced composites. J. Mech. Phys. Solids 37, 381–393.

Atkinson, C., 1975. Some results on crack propagation in media with spatially varying elastic moduli. Int. J. Fract. 11, 619–628.

Babaei, R., Lukasiwicz, S.A., 1998. Dynamic response of a crack in a functionally graded material between two dissimilar half planes under antiplane shear impact load. Engng. Fract. Mech. 60, 479–487.

Churchill R.V., Brown J.W., 1978. Fourier Series and Boundary Value Problems. 3rd edition, McGraw-Hill, New York.

Ding, K., Weng, G.J., 1999. The influence of moduli slope of a linearly graded matrix on the bulk moduli of some particle and fiber-reinforced composites. J. Elast. 53, 1–22.

Duan Z., Li, C., Zou, Z., 2001. Advances in fracture mechanics of functionally graded materials. J. Adv. Mech., in press (in Chinese).

Erdogan, F., 1975. Complex Function Technique. Continuum Physics, vol. II, Academic Press, New York, 523–603.

Erdogan, F., 1995. Fracture mechanics of functionally graded materials. Compos. Engng. 5, 753–770.

Erdogan, F., Wu, B.H., 1995. Crack problem in FGM layers under thermal stresses. J. Thermal Stresses 19, 237–265.

Jasiuk, I., Kouider, M.W., 1993. The effect of an inhomogeneous interphase on the elastic constants of transversely isotropic composites. Mech. Mater. 15, 53–63.

Li, C., Zou, Z., 1999a. Torsional impact response of a functionally graded material with a penny-shaped crack. J. Appl. Mech. 62, 566–567.

Li, C., Zou, Z., Duan, Z., 1999b. Torsional impact response of a transversely isotropic solid with functionally graded moduli and a penny-shaped crack. Theoret. Appl. Fract. Mech. 32, 157–163.

Miller, M.K., Guy, W.T., 1966. Numerical inversion of the Laplace transform by use of Jacobi polynomials. SIAM J. Numer. Anal. 3, 624–635.

Sneddon, I.N., 1972. The Use of Integral Transforms. McGraw-Hill Book Company, New York.

Tanigawa, Y., 1995. Some basic thermoelastic problems for nonhomogeneous structural materials. Appl. Mech. Rev. 48, 287–300.

Wacker, G., Bledzki, A.K., Chate, A., 1998. Effect of interphase on the transverse Young's modulus of glass/epoxy composites. Composites 29A, 626–629.

Wang, X.D., Meguid, S.A., 1995. On the dynamic crack propagation in an interface with spatially varying elastic properties. Int. J. Fract. 69, 87–99.

Wang, B., Han, J., Du, S., 1998. Dynamic fracture mechanics analysis for composite material with material nonhomogeneity in thickness direction. Acta Mechanica Solida Sinica 11, 84–93.